NUM
02

INTERNATIONAL JOURNAL OF **NUCLEAR MEDICINE** AND MOLECULAR IMAGING

THE NUCLEAR MEDICAL **SPECIALIST IN MEXICO:** CONSULTANT AND EXECUTOR A PATH OF CONTINUOUS IMPROVEMENT

VOL 2 + MAY - AUGUST 2015

EDITORIAL

THE NUCLEAR MEDICAL SPECIALIST IN MEXICO: CONSULTANT AND EXECUTOR A PATH OF CONTINUOUS IMPROVEMENT

Nuclear medicine was first practiced in Mexico 50 years ago. Half a century of constant effort and renovation have brought several of those more directly involved (myself included) to reflect upon the role that the nuclear specialist has played throughout this period. The kind of expert we refer to shares the responsibility with leaders of other disciplines to expound upon, teach and offer opinions regarding the benefits of their respective fields. From this position the nuclear specialist is in fact a medical opinion leader whose evolution and perfecting cycles have drawn him closer to modern definitions of efficiency and efficacy, which in turn renders task of producing optimal results during the medical process more feasible. Such characteristics have also made this kind of expert a highly suitable consultant and grant the authority required to decide upon the type of study, method and timeframe to be applied when called for.

As an instructor who masters his field and guides new specialists using a wide range of ground-breaking resources, the expert in nuclear medicine must always remain aware of the close relationship and constant interaction that exists between this discipline and other scientific fields such as physics, engineering and molecular bio-chemistry, among several others. He or she will define the form and direction an investigation takes and apply any advances and technological innovations that are available for basic research as well as for daily use with patients, while also setting aside enough time to produce scientific articles of the highest quality.

The tradition that was started by the honorable founders of this specialty has been handed down from generation to generation, and this tradition consists in: learning, carrying out, experimenting, consulting, analyzing, writing, teaching, and what is most astonishing of all, in doing these things simultaneously -which includes seeing to medical matters as well as those of an administrative and normative nature. The role has thus given rise to a new type of doctor, one who is unique within the larger scope of the disciplines we are referring to.

Year after year new achievements have crystalized. In the beginning, the number of physicians and medical service professionals in this country who were specialized in the field was scarce, to say the very least. Today, on the other hand, we have resident doctors preparing for this line of expertise as well as other areas of medicine and research: Growth has been continuous both in terms of quantity and quality, while different divulging channels such as The Journal are now available to help bring us closer to the goal we have firmly set ourselves, that of projecting our work internationally; this publication has become the medium for global dissemination of nuclear medicine specialists working in Mexico.

Let us therefore rejoice in the celebrations of our 50th anniversary, for I am certain that it will spur on nuclear medical specialists toward new horizons and give them fresh inspiration to continue opening pathways for the benefit of patients, institutions and country alike.

DRA. GRACIELA VILLALOBOS BENITEZ
PRESIDENTE DE LA FEDERACION MEXICACA DE MEDICINA NUCLEAR

INDEX

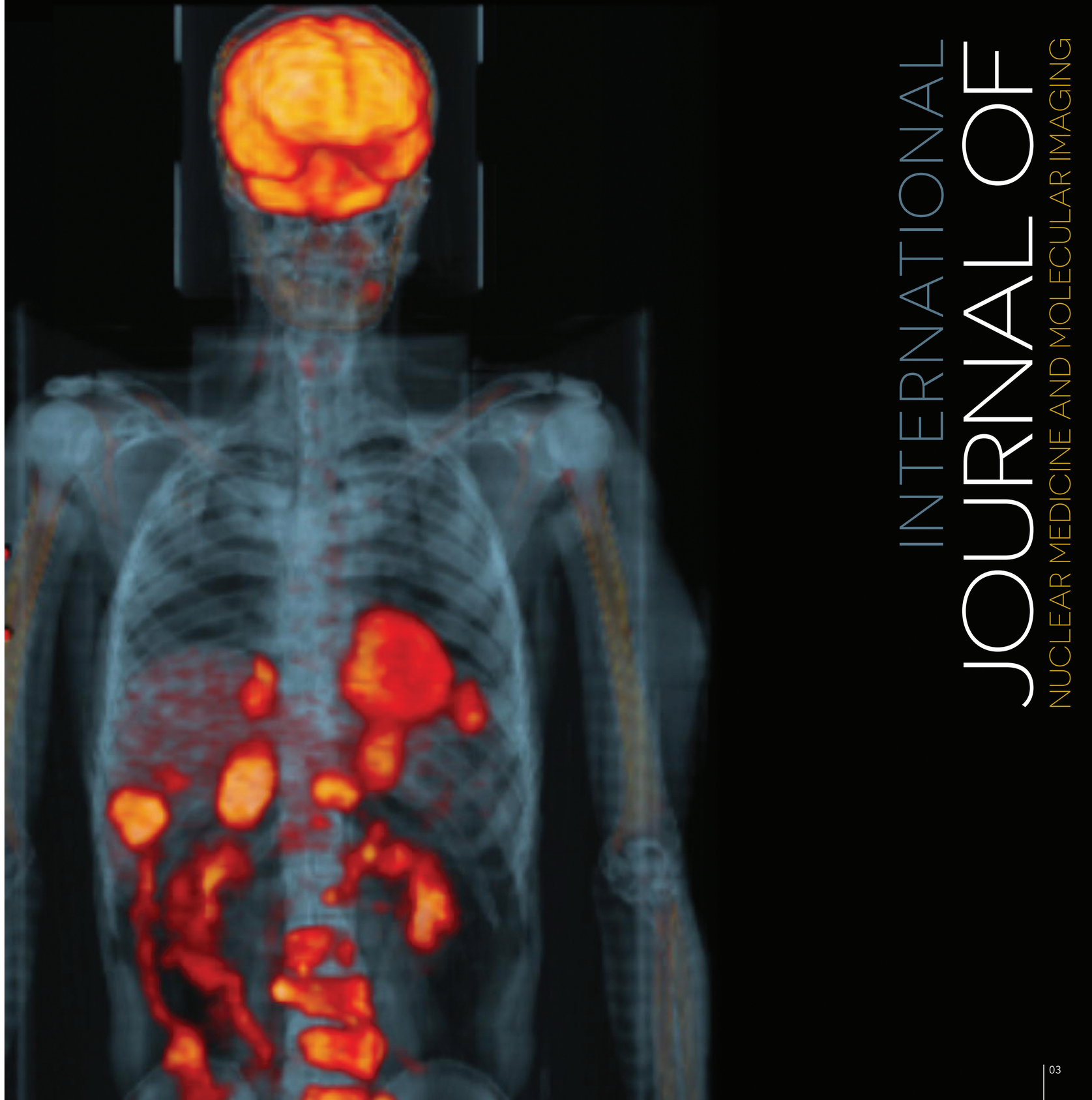

INTERNATIONAL JOURNAL OF NUCLEAR MEDICINE AND MOLECULAR IMAGING

REVIEW ARTICLES

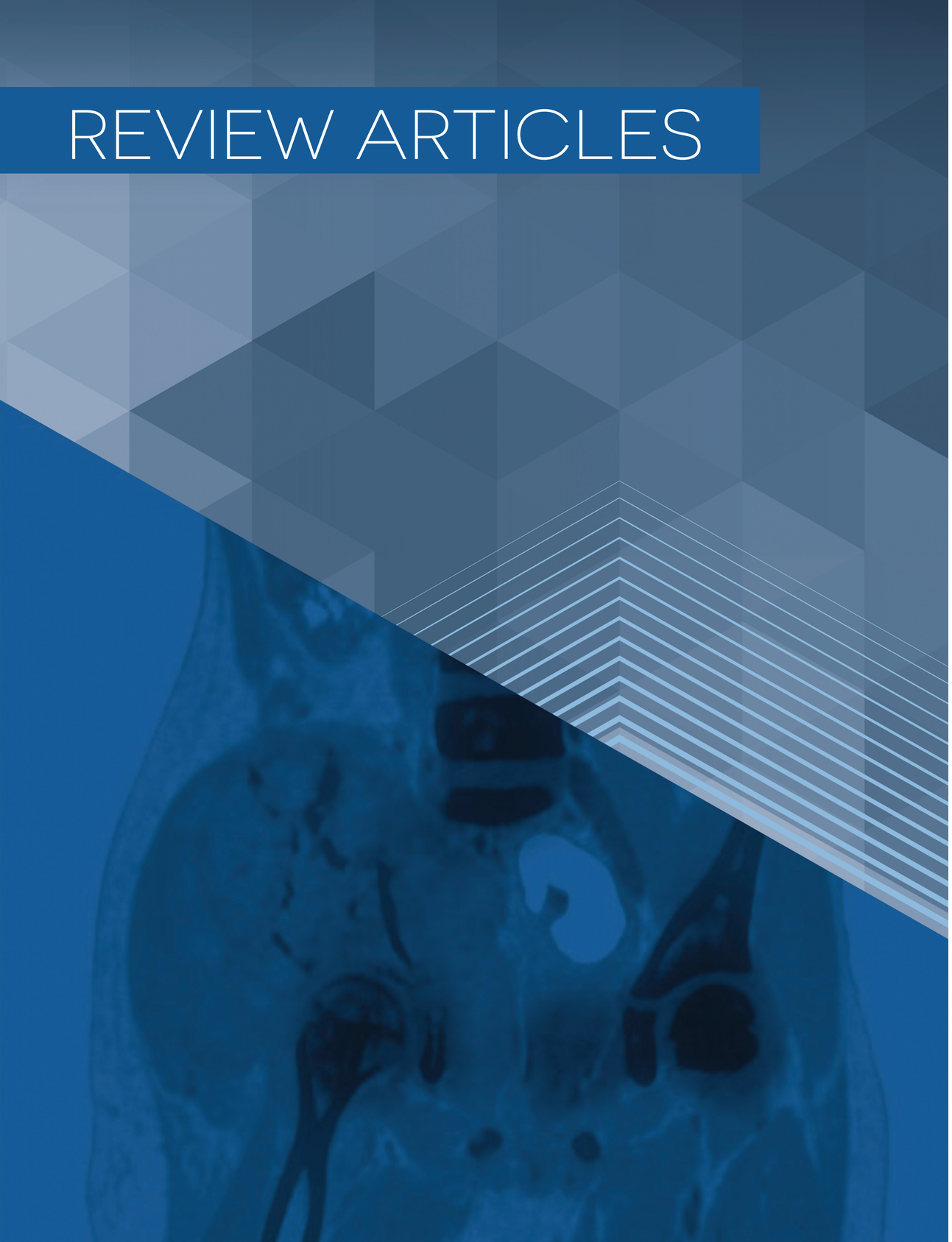

99MTC UBIQUICIDIN (99MTC UBI) FOR THE DIAGNOSIS OF OSTEOMYELITIS

Nudelman-Speckman Amandaa, García Pérez Osvaldob.

Osteomyelitis is an inflammatory process accompanied by bone destruction caused by an infecting microorganism. The infection can be limited to a single portion of the bone or can involve several regions, such as marrow, cortex, periosteum, and the surrounding soft tissue . Although there have been several medical and surgical advances in the areas of orthopedics and traumatology, the bone infections represent difficult diagnosis and management, with a strong tendency to become a chronic condition that affects the quality of life of the patients and their family, with a strong impact on health systems. (1-3, 4).

It is recognized that in the epidemiology of this disease there is an interaction between the host, the agent and the environment. In a study conducted in Mexico in 2002 by researchers at the National Institute of Rehabilitation (INR), with a sample of 202 patients.

It was identified that in our population the main risk factors for developing this disease are men (3:1 male/female ratio), aged in the third decade of life; with predominant mechanisms of infection such as the presence of previous injury produced by a fall and by traffic accidents. The main risk factors associated with this disease were identified; some being gender (3:1 male/female ratio), age (predominantly in the third decade of life) and infection prone situations such as previous injuries produced either by falls or vehicular accidents. The most affected regions were the tibia (37%), femur (19%), humerus, radius and ankle bones. In 52% of cases the duration of infection was longer than 12 months .

In addition to the above mentioned factors other, as equally important due to their prevalence in the Mexican population are: diabetes mellitus, alcoholism, intravenous drug use, pre-existing bone diseases, prosthesis, chronic steroid use and immunosuppression.

The main pathogens involved in over 50% of cases are Staphylococcus aureus and coagulase-negative Staphylococci; and to a lesser extent (25%) Streptococci, Pseudomonas spp, Enterobacter spp, E. coli, Serratia spp, and anaerobic microorganisms (Peptostreptococcus, Clostridium and Bacteroides) .

The virulence factors that are associated with this type of infection are the capacity of adhesion to the bone, biofilm formation, loss of immune response, production of catabolic factors from bone matrix cells such as exotoxins, hydrolases and proteases, the promotion of degradation processes and the inhibition of the regeneration of new tissue.

In osteomyelitis of any kind, the most important step is to isolate the offending organisms so that the appropriate antimicrobial therapy can be chosen. Isolation can be achieved by blood cultures or by a direct biopsy from the involved bone. Laboratory tests, such as the white blood cell count, concentration of C-reactive protein and erythrocyte sedimentation rate, may not be reliable indicators considering that they might be normal or elevated due to reasons other than osteomyelitis.

Imaging procedures have a confirmatory role. Standard radiography, magnetic resonance imaging (MRI) and computed tomography (CT) are commonly used to detect inflammatory and infectious bone lesions. Although MRI and CT have excellent resolution power and can reveal the destruction of medulla as well

as periosteal reactions, cortical destruction, articular damage, and soft-tissue involvement, they might not be useful for early infection , considering that the alteration of anatomic structures may take days to become evident. Also, it is important to notice that, in the presence of distortion of the normal anatomy, i.e., post surgical changes, scarring, prosthetic joints or metallic implants, and also in chronic infections, the diagnostic role of these techniques is limited .

Nuclear Medicine identifies the physiological/biochemical molecular response to a pathogen, prior to secondary structural changes achieving a positive impact on patient prognosis. In this sense, whole body scans, combined with tomography and hybrid SPECT/CT imaging allow:

- Early diagnosis of infectious process.
- Discrimination between active processes and pre-existing anatomical changes.
- Location of the number and size of lesions.
- Determination of the involvement of the different compartments.
- Conducting diagnostic intervention or treatment; with assessment of response to therapy.

For this purpose, multiple radiotracers have been developed considering the multiple mechanisms in the infectious process, such as: increased capillary permeability, vasodilation and hyperemia that favor the arrival of the radiopharmaceutical; specific molecular targets in inflammatory cells and their products; and targeted directly against the pathogen.

Unfortunately, none of the current available radiopharmaceuticals, e.g., gallium-67-citrate, 111In and 99mTc-labelled autologous leukocytes, or even 18F-FDG distinguishes between infection and sterile inflammation

The development of new radiopharmaceuticals for infection is based on the need to find options that present a unique tissue uptake (scintigraphic image) in the context of infection and a negative image in aseptic inflammation or tumor pathology. With this purpose, the labeling with 99mTc for antibiotics has been investigated with different results. Also, multiple peptides have been developed for the identification of non-oncological disease . This research reviews what has been published for osteomyelitis with 99mTc ubiquicidin [29-41] (99mTc-UBI)

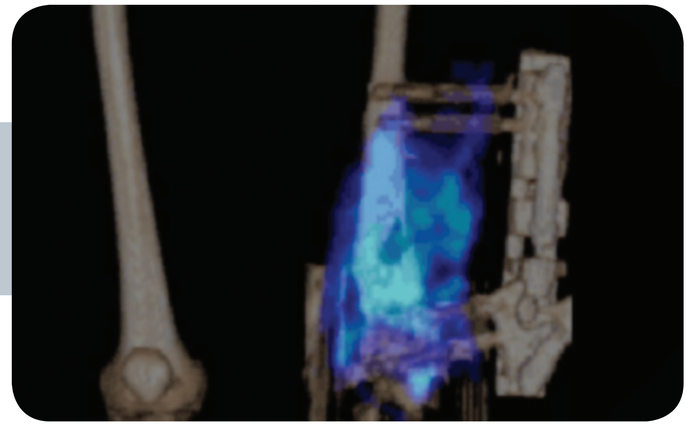

Figure 1: SPECT / CT study of a patient with infection associated to fastening material, in which focal radiotracer uptake seen in bone and soft tissue is consistent with osteomyelitis (INCan, 2012).

FEATURES OF UBIQUICIDIN

Ubiquicidin is a member of a range of antimicrobial peptides such as lactoferrin and defensins, which are an important form of humor immune response in multiple animal and vegetal species . This molecule is composed of hydrophobic amino acids with cationic charge organized in an amphipatic a helix structure. This antimicrobial peptide displays activity against bacteria, viruses and fungi by destabilization and perforation of the cell membrane; and also their intercellular activity leads to disturbed metabolic processes by inhibiting DNA synthesis and reducing mitochondrial metabolism .

Ubiquicidin was isolated from the cytosol of IFNy-activated murine macrophages, as part of their non-oxidative immune response, contained in vesicles along with lysozymes, defensins and serprocidins. In murine models, the bactericidal action of this peptide, in cultures of Listeria monocytogenes, is similar to the defensin NP-1 .

For diagnostic imaging purposes, it is preferred to use fractions of this peptide, that bind with higher avidity to bacterial domains without exerting a bactericidal action. The peptidic fraction 29-41 (although also the 18-35 and 22-35 fractions have been studied) with the amino acid sequence TGRAKRRMQYNRR, and a molecular weight of 1,693 Da, is the one used for 99mTc labelling in Nuclear Medicine studies.

In the human being, ubiquicidin corresponds to the ribosomal protein S30, encoded in chromosome 11q13.1, which is translated simultaneously with the FUBI protein, which is involved in cell apoptosis via Bcl-G; and is inhibited by certain types of cancer (breast, prostate and ovarian), although the clinical implications of this have not yet been explored . In humans, no antimicrobial activity has been found for this peptide.

PATHOPHYSIOLOGICAL BASIS OF99MTC-UBIQUICIDIN [29-41] (99MTC-UBI) SCINTIGRAPHY

In an active infectious process, the main uptake of 99mTc-UBI is seen in regions where the hypervascularity, stasis and increased permeability favors the radiopharmaceutical extravasation. In the presence of micro-organisms, the cationic residues of the ubiquicidin molecule interact electrostatically with the anions of the phospholipids of the cell membrane forming strong bondsviii; allowing subsequent scintigraphic detection. About 1-4% of the injected dose of 99mTc-UBI accumulates rapidly in bacterial or fungal infected tissues.

It is important to notice that, in experimental studies with animals, the 99mTc-UBI showed no significant uptake in sterile inflammation sites, in the presence of their lipopolysaccharide target or even with heat-damaged bacteria ($P<0.01$) . This has led to the hypothesis that this molecule requires interaction with the living organism to form the mentioned bond . It has even been stated that the intensity of the uptake (target/non target relationship) is a function of the amount of viable pathogens at the site of infection . This relationship is maintained with a minimum number of bacteria of 103-104 ix.

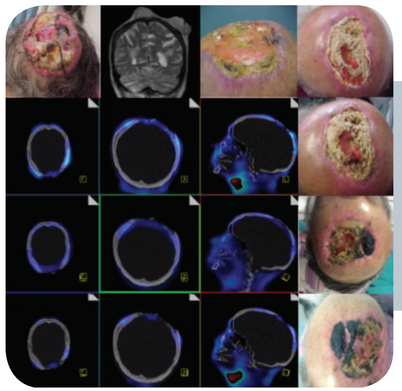

Figure 2: (A) 82 years old female, diagnosed with squamous cell cancer of the scalp. In MR imaging, there is no evidence of intracranial or meningeal involvement. She was treated with radiation therapy. However, the patient developed grade IV radiation necrosis with bacterial superinfection. Treatment was initiated with amoxicillin-clavulanate. Monitoring of the response was carried out with 99mTc-UBI [29-41] SPECT / CT, with initial image that shows focal uptake in the primary lesion (B) with diminished uptake in subsequent studies every 2 months (C and D) that correlates with the clinical improvement (last row). (INCan, 2013-2014).

In vitro studies, to evaluate the specificity of binding,showed that 87% of the labeled peptide was bound to S. aureus; while less than 4% was fixed in human cells (ACHN of renal adenocarcinoma and LS174T of colon cancer origin) . This biochemical find supports the fact that in mammalian cells, unlike bacteria, the negatively charged phospholipids are directed toward the cytoplasmic region of the cell membrane. . For fungal infections, the utility of 99mTc-UBI [29-41] was demonstrated by the research of Lupetti et al, in which this peptide detected infections of Candida albicans and Aspergillus fumigatus, with the capacity to discriminate infection from sterile inflammation ($P<0.05$). This radiolabeled peptide was also useful for monitoring the efficiency of antifungal therapy ($P<0.017$). The disadvantage is that it is not able to discriminate between fungal and bacterial infections .

Another aspect to note is that it has been shown that the uptake of 99mTc-UBI [29-41] is independent of the cellular immune response of the host, since the accumulation of the peptide in leukopenic mice showed no difference with those immunocompetentxii.

PHARMACOLOGICAL PROPERTIES OF 99MTC-UBI [29-41]

Antimicrobial peptide production is performed in genetically engineered bacteria, transgenic animals or by peptide synthesis. These techniques rendered sufficient amounts of antimicrobial peptides, under good laboratory practice conditions .

The direct labeling of ubiquicidin 29-41 with 99mTc is a simple method that results in the peptide complex. The amine residuals of the Arg and Lys of the ubiquicidin fragment are considered the most suitable binding sites for the radioisotope. This is a simple and fast procedure, with a relatively short reaction time of 10-20 minutes, with high labeling yield of more than 95%. The stability of this complex is reported to be excellent: less than 5% of free 99mTc in diluted human serum at 24 h and effective radiochemical purity of >97% , with conserved biological activity. Lyophilized labeling kits, developed by the International Atomic Energy Agency (IAEA) and the National Institute for Nuclear Research (ININ (Mexico), are already available in Mexico, with the same efficiency.

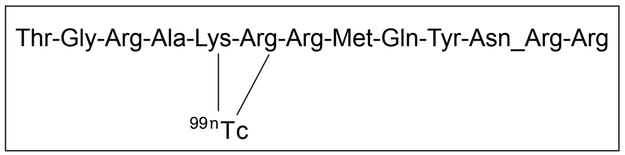

Figure 3: Structure of99mTc UBI [29-41] as proposed by Meléndez- Alafort et.al

As to safety, there has been no side effects reported in studies with 99mTc-UBI in human beings ; and it is thus considered a molecule with low immunogenicity. Even at high doses, this peptide has been well tolerated by mice and rabbits, without evidence of mortality, changes in body weight or alteration in the levels of serum leukocytesxviii.

Regarding the possibility of the absence of tracer uptake by the resistance of microorganisms to antimicrobial peptides, no evidence has been reported in the reviewed publications . It is considered that this resistance could be developed by pathogens by modifying the lipid composition of the cell membrane, increasing its virulence or with the production of proteases that can degrade these peptides .

CLINICAL APPLICATIONS OF 99MTC-UBI [29-41]

In human studies, 99mTc-UBI was reported to have a fast blood clearance with a mean residence time of 0.52 h, and 85% of the activity cleared by the bladder within 24 h of administration , conferring a low whole body dosimetry, the kidneys being the critical organ with 0.13mGy/MBqxv. Acquisition protocols may include three-phase studies obtaining adequate visualization of the site of infection from 30 minutes after injection. The highest definition of target/non-target (T/NT) is obtained at 120 minutes, with an average T/NT ratio of 2.18 ± 0.74xxv.

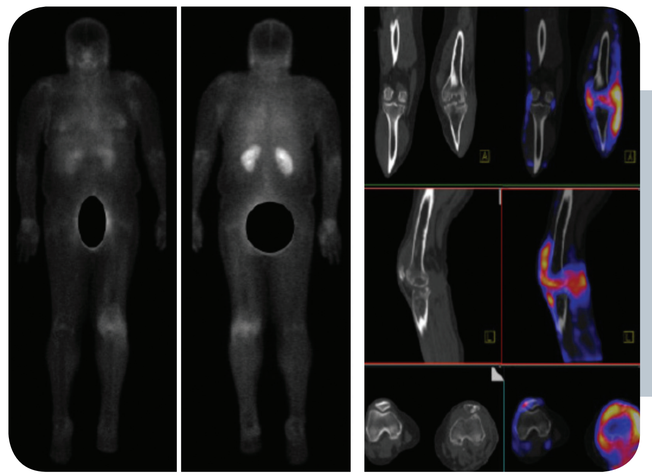

Figure 4: (A) whole body scan showing normal biodistribution and elimination route of 99mTc-UBI [29-41], with abnormal focal uptake in the left knee. (B) SPECT / CT shows that the uptake of the radiotracer includes bone and soft tissue at this level; with anatomical changes that are characterized by lytic destruction of the facet joint of the femur, tibia and patella, loss of muscle planes and striation of the fat, consistent with chronic osteomyelitis (INCan, 2013).

Limited, but promising, are the recently published pilot and clinical studies on 99mTc-UBI. Beiki et al reviewed 70 cases of patients with suspected osteomyelitis and infection of orthopedic implants, adding results of their hospital and previous studies, calculating rates of sensitivity and specificity of 100% and 90.4%, respectively, for the diagnosis of these pathologiesxxii.

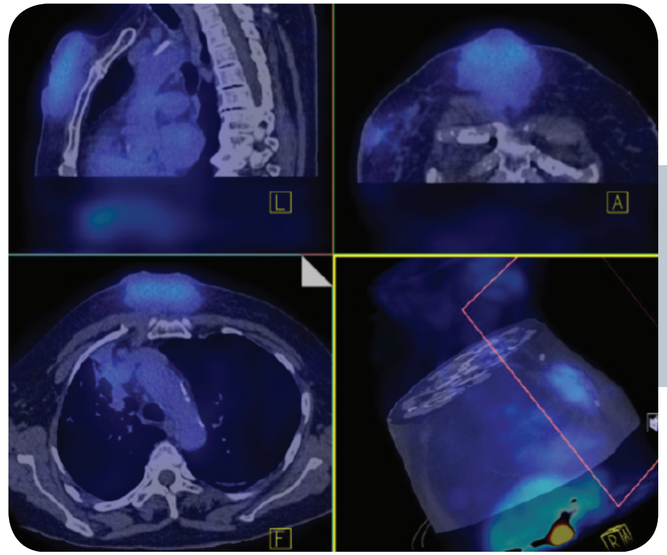

Figure 5: SPECT / CT with 99mTc-UBI [29-41] of a patient who underwent a mastectomy with subsequent infection of the chest wall. The focal uptake of the radiolabeled peptide in the soft tissue excluded the osseous involvement; confirming the diagnosis of cellulitis (INCan, 2014).

However, application of 99mTc UBI scintigraphy is not limited to musculoskeletal infection; but also for diabetic foot infection endocarditisxvi, fever of unknown origin , with very high absolute and relative frequencies.

CONCLUSION:

The use of radiolabeled peptides may provide improved imaging with the benefit of more rapid imaging results, greater ease of radiolabeling, and better target specificity compared with current techniques. As we reviewed in this article, 99mTc-UBI has the following advantages:

- Application to a variety of infections, with the exception of intracellular microorganisms; which may be an advantage over radiolabelled antibiotics that target a limited spectrum of pathogens. No resistance to radiolabeled peptides has been observed to date.
- Allows the proper determination of the extent of the disease, to distinguish, through images of SPECT and hybrid studies, the involvement of soft tissue and bone.
- Useful in immunocompromised patients or in chemotherapy treatment.
- Supports the diagnosis of infection associated with prosthetic joints.
- Allows assessment of response to treatment in serial images.
- Detection of fungal infections by Candida albicans and Aspergillus fumigatus.
- Comfortable and safe acquisition protocol for patients.

REFERENCES

Lew DP, Waldvogel FA, "Osteomyelitis", Lancet 2004; 364:369-370.

Ramírez-Pérez S, Tirzo A León S, "Perfil socioeconómico y epidemiológico del paciente con infección ósea, informe de 202 casos", Rev Mex Ortop Traum 2002; 16(3): 155-160.

Chihara S, Segreti J, "Osteomyelitis". Dis Mon 2010: 66:6-31

Palestro CJ, Love C, Miller TT. "Imaging of musculoskeletal infections", Best Practice & Research Clinical Reumatology 2006.

Love C, Palestro C. "Radionuclide imaging of inflammation and infection in the acute care setting", Semin Nucl Med 2013; 43:102-113.

Knight LC, "Non-oncologic applications of radiolabeled peptides in nuclear medicine", Q J Nucl Med 2003; 47:279-291.

SaeedA,BabarM,AfzalM,et.al."Reviewarticle:Antimicrobialpeptidesasinfectionimagingagents:Betterthanradiolabeled antibiotics", Hindawi Publishing Corporation, International Journal of Peptides, 2012.

Otvos L, "Antibacterial peptides and proteins with multiple celular targets", J Pept Sci, 2005; 11: 697-706.

Hiemstra PS, Van den Barselaar MT, Roest M, et.al. "Ubiquicidin, a novel murine microbicidal protein present in the cytosolic fraction of macrophages", Journal of Leukocyte Biology 1999; 66:423-428

Pickard, M. "FAU (Finkel-Biskis-Reilly murine sarcoma virus (FBR-MuSV) ubiquitously expressed)", Atlas Genet Cytogenet Oncol Haematol, 2012; 16(1): 12-17.

Welling MM, Ferro-Flores G, Pirmettis I, Brouwer C. "Current Statutus of imaging infections with radiolabeled anti-infective agents", Anti-Infective Agents in Medicinal Chemistry, 2009; 8 (3):272-287.

Welling MM, Lupetti A, Balter HS, et.al. 99m-Tc labeled antimicrobial peptides for detection of bacterial and Candida albicans infections", J Nucl Med 2001; 42;788-794.

Saeed A, Iqbal J, Hkan M, et.al. "99m Tc labeled antimicrobial peptide ubiquicidin (29-41) accumulates less in Escherichia coli infection tan in Staphlococcus aureus infection", J Nucl Med 2004; 45:849-856.

Brouwer C, Gemmel F, Welling MM. " Evaluation of 99m Tc-UBI 29-41 scintigraphy for specific detection of experimental multidrug-resistant Staphylococcus aureus bacterial endocarditis", Q J Nucl Med 2010; 54(4);442-450

Ferro-Flores G, Arteaga de Murphy C, Pedraza-López M, et.al. "In vitro and in vivo assesment of 99m Tc UBI specificity for bacteria", Nucl Med Biol, 2003; 30(6):597-603.

Hancock REW, Scott MG. "The role of antimicrobial peptides in animal defenses", Proc Natl Acad Sci 2000; 97:55.

Lupetti A, Welling MM, Pauwels EK, Nibbering PH."Detection of fungal infections using radiolabeled antifungal agents", Curr Drug Targets, 2005; 6(8):945-954.

Lupetti A, Pauwels EKJ, Nibbering PH, Welling MM. "99m Tc- Antimicrobial peptides: Promising candidates for infection imaging", Q J Nucl Med 2003; 47:238-245.

Crudo JL, Nevares NN, Zapata AM, et.al. "Un estudio completo sobre la obtención de 99mTc-UBI 29-41 y su comportamiento in vitro e in vivo: su potencial uso en imágenes de infecciones", Alasbimn Journal 2005;7(28)

Ferro-Flores G, Arteaga de Murphy C, Melendez-Alafort L, et.al. "Molecular recognition and stability of 99mTc UBI 29-41 based on experimental and semiempirical results", Appl. Radiat. Isot, 2004: 61: 1261-1268.

Melendez-Alafort L. Ramirez Fde M. Ferro-Flores G. Arteaga de Murphy C. Pedraza-Lopez M. Hnatowich D.J. "Lys and Arg in UBI: a specific site for a stable Tc-99m complex?" Nucl Med Biol 2003;30(6):605–15.

Beiki D, Yousefi G, Fallahi B, et.al. "99m Tc-ubiquicidin 29-41, a promising radiopharmaceutical to differentiate orthopedic implant infections from sterile inflammation", Iranian Journal of Pharmaceutical Research, 2013, 12(2): 347-353

Ostovar A, Assadi M, Vahdat K, et.al. "A pooled analysis of diagnostic value of 99m Tc-ubiquicidin (UBI) scintigraphy in detection of an infectious process", Clin Nucl Med 2013; 38(6):413-416

Peschel A. "How do bacteria resist human antimicrobial peptides?", Trends Microbiol, 2002; 10:179-186

99mTc-Ubiquicidin29-41, Molecular Imaging & Contrast Agent Database.

Saeed S, Zafar J, Khan B, et.al. "Utility of 99m-Tc labelled antimicrobial peptide ubiquicidin (29-41) in the diagnosis of diabetic foot infection", Eur Nucl Med Mol Imaging 2013; 40(5):737-743.

Taghizadesh M, Mandegar M, Assadi M, "Technetium-99m-ubiquicidin scintigraphy in the detection of infective endocarditis", Hell J Nucl Med 2014; 17(1);47-48.

Sepúlveda-Mendez J, Arteaga de Murphy C, Rojas-Bautista JC, Pedraza-López M, "Specificity of 99mTc-UBI for detecting infection foci in patients with fever in study", Nucl Med Commun 2010; 31:889-895.

Ferro-Flores G, Arteaga de Murphy C, Pedraza-López M, Meléndez-Alafort L, Zhang YM, Ruscowski M, Hnatowich DJ. In vitro and in vivo assesment of 99mTc-UBI specificity for bacteria. Nucl Med Biol. 2003; 30(6):597-603.

Meléndez-Alafort L, Ramírez F M, Ferro-Flores G, Arteaga de Murphy C, Pedraza-López M, Hnatowich DJ. Lys and Arg in UBI: A specific site for a stable Tc-99m complex? Nucl Med Biol. 2003; 30:605-615.

Meléndez-Alafort L, Rodríguez-Cortés J, Ferro-Flores G, Arteaga de Murphy C, Herrera-Rodríguez R, Mitsoura E, Martínez-Duncker C. Biokinetics of 99mTc-UBI 29-41 in humans. Nucl Med Biol. 2004; 31: 373-379.

Ferro-Flores G, Ramírez F de M, Meléndez-Alafort L, Arteaga de Murphy C, Pedraza-López M. Molecular recognition and stability of 99mTc-UBI 29-41 based on experimental and semiempirical results. Appl Radiat Isot. 2004; 61: 1261-1268.

Ferro-Flores G, Arteaga de Murphy C, Palomares-Rodríguez P, Meléndez-Alafort L, Pedraza-López M. Kit for instant 99mTc labeling of the antimicrobial peptide ubiquicidin 29-41. J Radianal Nucl Chem. 2005; 266:307-311.

3 FACTORS AFFECTING STANDARD UPTAKE VALUE (SUV) QUANTIFICATION IN PET SCANS

Héctor Alva-Sánchez.
Unidad de Imagen Molecular PET/CT, Instituto Nacional de Neurología y Neurocirugía Manuel Velasco Suárez, Insurgentes Sur 3877 Col. La Fama, 14269, México D.F., México. Email: halva@ciencias.unam.mx

ABSTRACT

The standard uptake value (SUV) is a measure to quantify radiopharmaceutical uptake, which takes into account injected activity and patient weight in user-defined regions of interest in positron emission tomography images. Its use and implementation during image analysis is relatively simple, while the magnitude can be influenced by a number of physical, technical and biological factors. This work is intended to create awareness of the multiple variables involved in quantitative analysis that have proven useful in differential diagnosis, patient cross-comparisons, follow-up scans and tumor recurrence assessment using the SUV. An in-depth understanding, close control and the inclusion of these factors in scanning protocols and image analysis allow for reproducible and reliable interpretations of PET studies.

KEYWORDS: Positron emission tomography, PET, standard uptake value, SUV, image analysis.

INTRODUCTION

Positron emission tomography (PET) scans provide useful functional and molecular information on organs, tissues or physiological processes depending on the radiopharmaceutical administered to the patient1. Traditionally and in its simplest form, PET scans have been used more as a qualitative tool in which visual evaluation of the tomographic image slices suffices to provide a diagnostic impression by nuclear medicine specialists of any given clinical entity. However, PET studies can and should be used in clinical practice as a quantitative or at least as a semi-quantitative, non-invasive imaging tool.

Quantification in PET scans consists in determining the amount of radioactive material uptake by different regions of a patient's body. Specifically, the intensity of a voxel (volume element) in a PET image should reflect the radioactivity concentration (radioactivity per unit volume) in the region studied. Regional quantification is affected by factors which depend on the patient's intrinsic health and by technical issues related to radiopharmaceutical administration and scanning procedures; likewise by the physics involved in the detection of annihilation photons, by image reconstruction and data processing, and by the image analysis itself. These factors take on particular importance when a reproducible and reliable quantification method is required, such as when making comparisons across different patients or in single patient follow-up studies, or with images acquired by different PET scanners.

The purpose of this work is to remind the nuclear medicine specialists of the existence of various parameters which, when kept under controlled and reproducible conditions, make PET scans a valuable and quantitative tool that provides useful and precise information for decision-making by the requesting physicians. Recognition of these factors will allow the nuclear medicine specialist to incorporate them into his/her comparisons and analysis during image interpretation, case evaluation and when giving diagnostic impressions.

Basically, image quality is characterized by three fundamental aspects: spatial resolution, contrast and noise. Spatial resolution can be described as the ability to identify small objects in an image, whereby the smallest physical dimensions of two objects in an image can be clearly identified as two distinct entities. In current PET technology, spatial resolution depends primarily on scanner-detector design and architecture. It is also limited by other physical processes, such as positron range before annihilation and by non-colinearity in terms of the direction taken by photons following positron annihilation. Likewise, spatial resolution depends on the radiopharmaceutical uptake region relative to the z-axis of the scanner, achieving the best performance for objects located at or close to the central axis. Modern PET systems typically provide spatial resolutions within the 4 to 5 mm range. Contrast refers to the ability to identify objects over a background with a distinct radiopharmaceutical uptake. In PET studies, contrast depends mainly on the volumetric distribution of the radiopharmaceutical and on the region of interest to the physician; it is further influenced by technical aspects like biodistribution timing and by the physics of photon detection such as the number and type of detected (i.e. scattered or random) events.

Noise relates to registered events that do not contribute to providing useful information from the image. Noise inherent to the random nature of radioactive decay and electronic noise in the equipment are always present in PET studies. There may also be structured noise caused by artifacts in the reconstructed image, due to patient motion or else caused by regions with high-activity concentrations in certain regions (e.g. bladder accumulation if the radiopharmaceutical has urinary excretion). It is not unusual to find that factors affecting image noise also have an impact on spatial resolution and contrast, and vice versa. In general, the larger the number of detected events for image formation, the better image quality is obtained. This reminds us of one of the biggest challenges in PET studies: how to obtain a good image quality using only a small amount of radioactive material while maintaining the metabolic process involved unaffected and keeping the radiation dose on patients low?.

Image formation in PET is a complex mixture of various processes, some of which cannot be fully controlled. Arriving at precise, reliable and reproducible quantification is an objective difficult to attain in daily clinical practice, although this goal should be pursued if protocol standardization is ever to be achieved. Acquiring a true understanding of the factors involved is indispensable to obtaining accurate interpretations, while disregarding these factors will limit the correct implementation of PET as a quantitative, diagnostic tool.

THE STANDARD UPTAKE VALUE

In PET images, the standard uptake value (SUV) is used to perform semi-quantitative intra- and inter-patient comparisons2. In a simplified way, the concept behind this value lies in the fact that the net uptake by a certain organ or tissue depends largely on the amount of radiopharmaceutical administered, as well as patient weight. In multiple patients with varying body mass or in a single patient weighing differently at separate time points, the activity concentration in one region may be very different when the same amount of radiopharmaceutical had been injected. To take into account this effect, the activity concentration is normalized by the injected activity and by the patient's body mass. That is, the SUV is determined by computing the ratio of the activity concentration a(t) in a region of interest expressed in (Bq/ml) divided by the injected activity Actinj (Bq) and normalized by body mass (kg):

$$SUV = \frac{a(t)}{ACT_{inj}/mass}$$

The notation used here for the activity concentration a(t) is to emphasize its dependence on biodistribution time t (the time period measured between injection and image acquisition). SUV generally refers to the average (SUVmean) pixel or voxel value in a given region or volume or interest, a quantity relatively insensitive to image noise. The maximum SUV value (SUVmax) is also used in the clinical practice, and is a quantity more sensitive to image noise, but less dependent on the region of interest chosen by the nuclear physician (provided the region of interest includes that pixel). The SUVmax is less observer-dependent and therefore easier to use. The SUVpeak combines both methods. The SUVpeak represents the pixel or voxel average with the highest value within a region or volume. In this way, the SUVpeak preserves the reproducibility of SUVmax while being less susceptible to image noise. Computing the SUVpeak is equivalent to smoothing an image and then measuring the SUVmax3. This

slightly more sophisticated and robust quantity has been proposed as the method of choice in the PERCIST (PET Response Criteria in Solid Tumors) criteria for assessment and monitoring of treatment response in oncology4. More rigorous and quantitative analysis of PET images can be performed, but these require dynamic scans acquired from the moment of radiopharmaceutical administration, as well as radioactivity measurements of blood samples and complex compartmental modeling5. Still, many of the factors described below may also have an impact on the more quantitative tools used in kinetic analysis.

BIOLOGICAL FACTORS

The SUV is influenced by a number of biological and patient related factors, such as hydration and metabolic status, applying particularly to 18F-2-deoxy-D-glucose ([18F]-FDG) studies. The specific condition of each patient should be considered when using other radiopharmaceuticals. Additional factors include the underlying physiopathology for each case, further diseases, fasting periods as well as physical or cognitive activity previous to the PET study. Patient age, constitution, blood glucose levels, anesthetics or other drugs that may influence the functional process to be evaluated also modify SUV results6.

Patient constitution is of utmost importance in [18F]-FDG PET scans7. Adipose tissue tends to have a lower uptake compared to lean tissue. Lesion uptake in an obese patient tends to be higher than in a person of average weight. Previous definitions of SUV do not take this effect into account; therefore the SUVlean corresponding to lean body mass in the denominator, which is estimated from the patient's weight and height, was introduced. This alternative definition is particularly valuable in patients whose weight has undergone significant changes along the treatment course, as commonly found in oncology. Furthermore, in two patients with the same body mass index but who differ considerably in height, lean body mass correction may be insufficient. In this case, the body surface area could prove more appropriate for SUV normalization8. In any case, it is always convenient to register both the patient's weight and height on the day of the PET scan and to be aware that these factors may substantially affect SUV determination. The appropriate choice of SUV definition may thus be crucial in making intra- and inter- patient comparisons.

High blood glucose and insulin levels may notoriously affect [18F]-FDG distribution and SUV values. For this reason, verifying glucose levels prior to a PET study is of utmost importance. If glucose levels are above 200 ml/dl, it is best to postpone the PET scan. SUV correction providing a factor proportional to glucose levels has failed to turn in reliable results. It is best, therefore, to reschedule the PET scan when glucose levels are within normal ranges.

[18F]-FDG biokinetcis relates directly to tissue uptake, which is different in regions with tumor activity compared to normal tissue9. In general, tumors continue to accumulate [18F]-FDG for longer time periods, while normal tissue tends to have stable levels, or even shows a decrease in activity concentration, as in the case of tissues expressing the glucose-1 phosphatase enzyme. Generally speaking, SUV values are higher in malign tumors in PET studies acquired following longer biodistribution times. For tumor differentiation it is best to ensure that PET scans with [18F]-FDG are performed at least 60 min after radiopharmaceutical administration. Naturally, this effect is useful for categorizing the etiology of an undetermined mass and to increase tumor-normal ratio10. Patient motion (including breathing and heart beat) may affect SUV quantification in thoracic regions. This is due to two main phenomena: first, motion introduces image smoothing whereby activity concentration values are distributed over larger volumes, which reduces SUV values; second, attenuation correction (described below) may also be incorrect. To minimize this effect, it is recommended to acquire the CT scan while the patient holds his/her breath during the exhaling phase.

PHYSICAL FACTORS

Activity concentration quantification is affected by several physical factors. In particular, it is affected by the attenuation of annihilation photons in the patient11 –all the more important in larger patients- and by the partial volume effect, which is related to the limited spatial resolution of the PET scanner, and bears greater importance with small objects.

Photon attenuation is the reduction of the number of detected events by the PET scanner due to complete absorption (photoelectric effect) or scattering (Compton scattering) in the patient. The method most frequently used to correct for attenuation consists in collecting a CT scan (in hybrid PET/CT systems) of the patient prior to PET acquisition. CT images reflect linear attenuation coefficients of the different tissues present in the body; these represent the probability of photon interaction with the material it encounters. This probability is related to physical density, effective atomic number (composition) and material thickness; it also depends on photon energy, with lower values with increasing photon energies. The correction factors along each line of response to compensate for 511 keV photon losses are obtained through a CT scan and introduced into the reconstruction algorithm. This correction, more difficult to perform in SPECT scans, is possible since attenuation correction factors are independent of the positron-electron annihilation location inside the patient12.

Although attenuation correction in PET/CT is satisfactory, it is not always accurate. This is due to the energy of the x-rays being lower than that of the annihilation photons; hence linear attenuation coefficient scaling to 511 keV is required. In addition, x-rays are not monoenergetic and this introduces an artifact in the CT images known as "cupping effect", which arises due to beam hardening13. Beam hardening is the result of a large fraction of low-energy photons being attenuated as the x-ray beam traverses the patient, causing a shift in the mean photon energy to higher values (image reconstruction in CT assumes a monoenergetic x-ray beam). All of this is finally reflected in inaccuracies in the corrected PET image. For reproducible results, both PET and CT (current, exposure time, kilovoltage and pitch) acquisition parameters should be kept the same.

As opposed to the photon attenuation problem, which is more important for large structures, the partial volume effect makes for imprecise quantification in smaller volumes. This is a consequence of the finite dimensions of scanner detectors. For objects with dimensions smaller than the detector elements, the corresponding image will show activity concentration values averaged over several adjacent pixels or voxels. In fact, if the object is two times smaller than the scanner's spatial resolution, then the SUV and the apparent object size will not be reliable14. The problem of SUV under-quantification resulting from the partial volume effect is particularly relevant during follow-up PET scans. A reduction in tumor size and uptake may be the result of both effective treatment and partial volume effect.

Another factor affecting spatial resolution in the reconstructed set of PET images, and thus SUV, is the photon depth of interaction in the scanner detectors. This is caused by a parallax error that inadequately assigns lines-of-response to the coincidence events. This effect is more important for objects placed further from the scanner's central axis, where quantification of lesions located at the periphery of the image may have lower SUV values. Both system dead time and random coincidence rates depend on the total amount of radioactivity placed in the scanner field of view. During system dead time, two distinct events are registered as a single event. Random coincidences refer to the various events registered simultaneously and results in misallocation events due to uncertainty in the line-of-response assignation made to annihilation events. The final result is a loss of events at high-counting rates. Therefore, in addition to keeping patient dose low, nuclear medicine technicians and nurses should endeavor to maintain injected activities low in order to preserve image quality for optimum interpretation.

All of these effects depend on the specific design and architecture of the PET scanner being used. This makes it difficult to make quantitative comparisons of SUV values from PET scans acquired using different PET units. Modern PET scanners with faster detectors, for example, incorporate time-of-flight information (time difference between annihilation photon pair detection) in order to provide better spatial resolution. This has shown comparatively higher SUV values in smaller lesions15. As the development of technology moves us toward higher detection efficiency and increased spatial resolution, we can expect to see larger SUV values in smaller hot regions with newer PET systems, thus increasing lesion detectability.

TECHNICAL FACTORS

The fundamental technical factors which can undermine accurate SUV measurements bear a close relationship to the amount of radiopharmaceutical that is administered. Errors in determining activity

prior to injection may accumulate if the well-counter, technician and PET system clocks are not synchronized. Also, residual activity in the syringe, needle and catheter should be measured and registered with the appropriate time. As previously mentioned, the SUV depends strongly on the time period between injection and scan start. In order for the effectiveness of a treatment to be assessed, it is important to keep biodistribution times within ± 20% for [18F]-FDG studies. Obviously, the well-counter should have a certified calibration and daily quality-control test with certified reference sealed sources should be performed. Needless to say, PET scanner calibration and performance should be verified by an experienced medical physicist.

Follow-up patients should ideally be weighed on the same calibrated scale prior to every PET scan. Patient weight and height must be introduced carefully to the system in an effort to minimize typing errors.

The use of an oral/intravenous iodine-based contrast medium for the CT scan in PET/CT studies may affect the SUV values, this due to the attenuation correction issue mentioned earlier. It should be clear by now that basal and follow-up scans must be performed keeping as many parameters as constant as possible and likewise it is strongly recommended to keep records of details regarding the parameters used for both PET and CT scans.

IMAGE RECONSTRUCTION FACTORS

Modern PET/CT systems offer a wide variety of reconstruction protocols. Filtered backprojection along with complex iterative-statistical algorithms to provide improved image quality are included. The iterative methods allow for image correction for photon attenuation and scattering. However, the optimum number of iterative steps and subsets required is not known and its choice will strongly depend on the pathology and equally on the technician and nuclear medicine specialists' experience and preference. Generally, image noise is increased with each additional iteration, affecting primarily the SUVmax. Figure 1 shows the SUVmean values (uncertainty-bars represent standard deviation) of the same cerebral PET scan reconstructed using 8 different protocols. This study was obtained with a Siemens Biograph mCT. As can be seen, variations in SUVmean quantification are below 3%.

The image display matrix size plays an important role in image quality in terms of spatial resolution and contrast-to-noise ratio. This is due to the partial volume effect discussed earlier, occurring here, however, during image processing, reconstruction and image display. Again, these parameters should be kept constant. If raw data is still available (which takes up a large amount of disk space), image processing can be performed again when one is required to match scans with previous reconstruction parameters.

FACTORS TO BE CONSIDERED DURING IMAGE ANALYSIS

SUV quantification is invariably observer-dependent owing to region or volume of interest delimitation. Up to 17% variations in the SUVmean have been observed due exclusively to inter-observer variability. Care should be taken when setting a malignancy threshold (e.g. 2.5); the threshold must be determined for each PET scanner, ideally maintaining all acquisition variables fixed. Registration of SUVmax, SUVmean and SUV standard deviations is suggested prior to performing quantitative comparisons. The standard deviation may aid in verifying whether the PET/CT scans were collected under the same conditions. A noisier image (i.e. due to shorter scan times, longer biodistribution time-elapses or less injected activities) will have a larger SUV standard deviation16.

CONCLUSIONS

Quantitative PET/CT analysis is challenging but at the same time stimulating. However, when the nuclear medicine technician, medical physicist and nuclear medicine physician possess a thorough understanding of the technical subtleties that affect SUV quantification and, providing that all scans are taken under controlled conditions, if properly used this method will furnish the specialist with useful and reproducible information which makes it a valuable tool for diagnosis and follow-up.

ACKNOWLEDGEMENTS

The author would like to thank Iván E. Díaz-Meneses, MD for his revision of and comments on the manuscript and further to Nora E. Kerik-Rotenberg, MD for her support.

REFERENCES

1. Phelps ME. Positron emission tomography provides molecular imaging of biological processes. Proc Natl Acad Sci. 2000;97:9226-9233.

2. Thie JA, Understanding the Standardized Uptake Value, its methods, and implications for usage, J Nucl Med. 2004;45(9):1431-1434.

3. Adams MC, Turkington TG, Wilson JM, et al. A Systematic Review of the Factors Affecting Accuracy of SUV Measurements. AJR Am J Roentgenol. 2010;195:310-320.

4. Wahl RL, Jacene H, Kasamon Y, et al. From RECIST to PERCIST: evolving considerations for PET response criteria in solid tumors. J Nucl Med. 2009;50:122S-150S.

5. Watabe H, Ikoma Y, Kimura Y, et al. PET kinetic analysis-compartmental model. Ann Nucl Med. 2006;20(9):583-588.

6. Keyes J W Jr. SUV: Standard Uptake or Silly Useless Value? J Nucl Med. 1995;36:1836-1839.

7. Paquet N, Albert A, Foidart J, et al. Within-Patient Variability of 18F-FDG: Standardized Uptake Values in Normal Tissues. J Nucl Med. 2004;45(5):784-788.

8. Kim CK, Gupta NC, Chandramouli B, et al. Standardized uptake values of FDG: body surface area correction is preferable to body weight correction. J Nucl Med. 1994;35:164-167.

9. Jadvar H, Alavi A and Gambhir SS. 18F-FDG uptake in lung, breast, and colon cancers: molecular biology correlates and disease characterization. J Nucl Med. 2009;50:1820-1827.

10. Spence AM, Muzi M, Mankoff DA, et al, 18F-FDG PET of Gliomas at Delayed Intervals: Improved Distinction Between Tumor and Normal Gray Matter, J Nucl Med. 2004;45:1653-1659.

11. Bleckmann C, Dose J, Bohuslaviski K, et al. Effect of attenuation correction on lesion detectability in FDG PET of breast cancer. J Nucl Med. 1999;40(12):2021-2023.

12. Zaidi H and Hsegawa B: Determination of the Attenuation Map in Emission Tomography. J Nucl Med. 2003;44:291-315.

13. Barret FJ, Keat N. Artifacts in CT: Recognition and Avoidance. RadioGraphics. 2004;24:1679-1691.

14. Cherry SR, Sorenson JA and Phelps ME. Physics in Nuclear Medicine. 3rd edition. USA: Sauderns; 2003.

15. Karp JS, Surti S, Daube-Witherspoon ME and Muehllehner G. The benefit of time-of-flight in PET imaging: Experimental and clinical results. J Nucl Med. 2008;49(3):462-470.

16. Visser EP, Boerman OC and Oyen WJG. SUV: From Silly Useless Value to Smart Uptake Value. J Nucl Med. 2010;51:173-175.

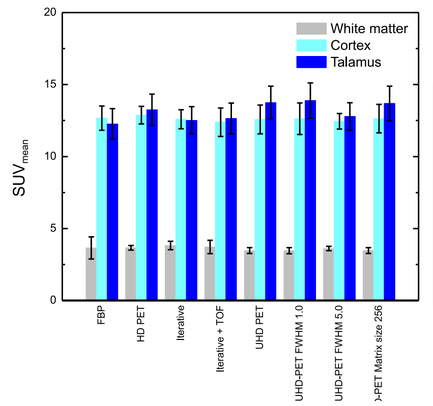

Figure 1. SUVmean for three regions of interest in a cerebral PET/CT scan with [18F]-FDG, reconstructed using different parameters. FBP: filtered backprojection; HD PET: high definition PET; TOF: time-of-flight; UHD: ultra-high definition; FWHM: full-width at half-maximum.

REPORT CASES

THE UTILITY OF HEPATOBILIARY SCINTIGRAPHY WITH 99MTC-MEBROFENIN IN THE EVALUATION OF CHOLEDOCHAL CYST: CASE REPORT

Gretty Tatiana Tapia Vega Second Year Resident of Nuclear Medicine. Herlinda Vera Hermosillo MN, Rafael Delgado Espín MN.
Hospital Infantil de México Federico Gómez.

INTRODUCTION

Choledochal cysts are congenital bile duct anomalies. These cystic dilatations of the biliary tree can involve the extrahepatic biliary radicles, the intrahepatic radicles. Population prevalence estimates of choledochal cysts range from approximately 1 case in 13,000 people to 1 case in 2 million people, more common in Japan and Asia, and frecuent in females1y5. The exact cause of the choledochal cyst remains obscure1. Several theories have been postulated, as follows: Weakness of the wall of the bile duct, obstruction of the distal choledochus, combination of obstruction and weakness, reflux of pancreatic enzymes into the common bile duct secondary to an anomaly of the pancreaticobilliary junction3. Clinical presentation: There is a classic triad: pain, jaundice, and a palpable mass in the right side of the abdomen1.

CLASSIFICATION (TODANI)3

Type I	Cystic or fusiform dilatation of the common bile duct (CBD); most frecuent type (90-95%)
Type II	Diverticulum of the common bile duct, with normal size CBD.
Type III	Choledochocele, a cystic dilatation of the distal intramural portion of the CBD, typically protruding into the second portion of the duodenum.
Type IV	Cystic or fusiform dilatation of the CBD associated with cystic, fusiform, or saccular dilatation of intrahepatic bile ducts, also termed form fruste
Type V	Cystic, fusiform, or saccular dilatation of the intrahepatic bile ducts associated with a normal CBD; may be associated hepatic fibrosis (referred to as Caroli disease).

DIAGNOSIS

Laboratories (blood count, liver function studies, serum amylase, lipase levels and serum chemistry levels). Imaging studies (Ultrasonography, abdominal computed tomography scanning and magnetic resonance imaging, magnetic resonance cholangiopancreatography1. Treatment: Surgery; is complete excision with construction of biliary-enteric anastomosis to restore continuity with the gastrointestinal tract2y4.

CASE REPORT

Female patient , 1 year and 2 months old, begins its condition 1 month previous with abdominal mass associated with crampy abdominal pain, plus constipation, evacuations every third day. Subsequently

diarrea one week of evolution, associated with pallor of teguments, hiporexia, general malaise attack, unspecified weight loss and abdominal volumen increase. Physical examination: palpable tumor of aproximately 10x8x10 cm, minimum displacement, apparently dependent of right upper quadrant. Abdominal tomography is performed, which shows tumor mass of cyst appearance, apparently dependent of choledochal, however it is not conclusive for choledochal cyst, therefore request complement with biliary tract scintigraphy, for definitive diagnosis. Hepatobiliary scintigraphy: The studies were performed in gamma camera Siemens Symbia T6 device. Sequential study of 60 seconds frames for 60 minutes with a 128x128 matrix was performed inmediately after intravenous administration of 99mTc-Mebrofenin (1mCi): shown adequate passage of radiotracer by large vessels and suitable extraction by hepatic gland, which shows a photopenic area adyacent to the liver. Sequential images showed radiotracer uptake in intrahepatic biliary tract showing no vesicular structure and with elimination to intestine. Subsequently delayed images acquisition (4 hours), shown radiopharmaceutical uptake by intrahepatic bile ducts and filled by common bile duct, where in topography of the site a round image is observed, that similarly concentrated radiopharmaceutical.

For morphologic correlation is performed tomographic techinique SPECT, 96 proyections, 30 seconds per projection, LEHR collimator, with subsecuent reconstruction. Tomographic images were fusion (SPECT/CT), show rounded picture and homogeneous appearance that depends on the common bile duct, liquid density having intense increased uptake of radiopharmaceutical. The structure already mentioned displaces the right kidney and intestinal structures, has dimensions in its longitudinal axis of 12.7 cm. Dilatation of the intrahepatic biliary its shown. Scintigraphic with functional compatible data for the presence of giant choledochal cyst.

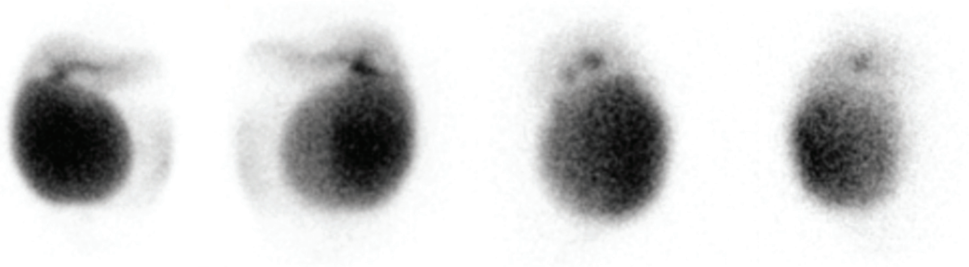

Static image in anterior projection

Static image in posterior

Static image in right lateral

Static image in left lateral projection

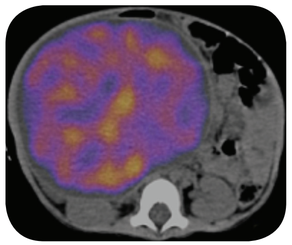

SPECT/CT axial section

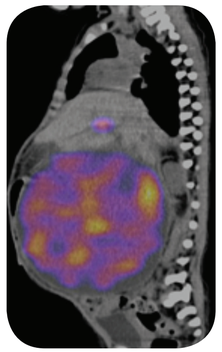

SPECT/CT sagital section

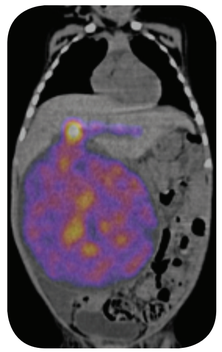

SPECT/CT coronal section

DISCUSSION

The diagnosis of choledocal cyst is usually suggested by clinical information and conventional radiographic evidence of displacement of adjacent organs by a cystic mass. 99m Tc-IDA cholescintigraphy allow specific preoperative diagnosis of choledochal cyst and may reduce the need for invasive studies. Also shows technical superiority by demostrating anatomy and function of the cyst. The use of scintigraphy with 99mTc-Mebrofenin in most of articles of case report where confiramtory or complemetary for this entity, which shows a clear progress of molecular imaging of seeking high diagnostic specificity for choledochal cyst. It allows us elucidate, not only utility, but also the added value that can provide this type of entities.

CONCLUSION

The molecular approach of biliary tract scintigraphy with 99mTc-Merbrofenin shows a clear example in increasing the specificity of diagnosis for choledochal cysts like in this case, which translates a therapeutic approach directed in these patients where conventional imaging techniques (CT),where inconclusive. We propose this method as an effective application as a complementary technique in clinical and therapeutic approach of this pathology.

BIBLIOGRAPHY

1.-Choledochal Cysts: Age of Presentation, Symptoms, and Late Complications Related to Todani's Classification, By J.S. de Vries, S. de Vries, D.C. Aronson, D.K. Bosman, E.A.J. Rauws, A. Bosma, H.A. Heij, D.J. Gouma, and T.M. van Gulik Amsterdam, The Netherlands, Journal of Pediatric Surgery, Vol 37, No 11 (November), 2002: pp 1568-1573.

2.-The Different Clinical and Liver Pathological Characteristics between the Newborns and Infants with Choledochal Cysts, Man-Chin Hua1,5, MD; Hsun-Chin Chao2, MD; Reyin Lien3, MD; Jin-Yao Lai4, MD; Ming-Wei Lai2,5, MD; Man-Shan Kong2, MD, Chang Gung Med J Vol. 32 No. 2 March-April 2009.

3.-Choledochal cysts, Janakie Singham, MD Eric M. Yoshida, MD Charles H. Scudamore, MD.From the Departments of Medicine and Surgery, the University of British Columbia, Vancouver, BC. J can chir, Vol. 52, No 5, octobre 2009.

4.-Tratamiento de los quistes de colédoco en la edad pediátrica, Dra. José David Palmer Becerra,* Dra. Patricia Ulloa-Patiño, Acta Pediatr Mex 2010;31(1):11-15.

5.- Reporte de un Caso Clínico, Quiste de Colédoco, Ibarra-jiménez Le, Ibarra-Capaceta L, Aguilar-Rendón TY, Fletes-kelly A, Flores-Arellano G, Sociedad Médica del Hospital General de Culiacán "Dr. Bernardo J. Gastélum" Arch Salud Sin Vol.5 No.2 p.51-54, 2011.

6.-Choledochal cyst: Diagnosis by Hepatobiliary Scintigraphy, I. frutos, m.d. Marín, M.e. Lillo, J. Coya, R. Couto, I.M. Martín Curto servicio de medicina nuclear.Hospital Universitario La Paz.Madrid.

7.-Quiste de colédoco, C. Pecharroman, A. Manrique, F. Arnaiz, C. Perez Qlgar, I. Cano.Hospital Universitario 12 Octubre)(Fetal Sonography and Neonatal Scintigraphy of a Choledochal Cyst Martha A. Wiedman, Anton Tan and Charles J. Martinez J Nucl Med. 1985;26:893-896.

8.-Choledochal Cyst with Bile Duct Dilatation: Sonography and 99mTcIDA Cholescintigraphy, Department of pediatrics Radiology, University of Cincinnati College of Medicine, Children's Hospital Medical Center, Cincinnati, OH 45229. Addre.

ROLE OF 18F-NAF DURING EVALUATION OF THE EFFICIENCY OF 4 DOSES OF 223RA WITH HORMONE-SENSITIVE PROSTATE CANCER: ORIGINAL CASE

Sevastián S. Medina-Ornelas y Francisco O. García-Pérez.
Department of Nuclear Medicine and Molecular Imaging, National Institute of Cancerology, Mexico.

INTRODUCTION

Based on data obtained from Globocan 2008, 14.217 patients are diagnosed with Prostate Cancer (PC) in Mexico each year, which corresponds to 11.7% of the new global tumor count in the country and places the disease first among men and women; men strictly rank first, accounting for 24.1% of recently diagnosed tumors [1,2].

A recently epidemiological study of PC in Mexico carried out by Sánchez-Barriga reported 51,389 deaths brought on by the disease during the period 2000-2010, where the gross mortality rate for men moved up from 7.8 to 9.8/100,000 while PC frequency and deaths caused by the PC also saw important increases in older age groups: 694 deceased were registered for persons aged 50-54 (1.3%), whereas those aged ≥60 reported 48,780 deaths, that is 94.9% of the total mortality count for the period studied [3]. Rizo et al reported that the neoplasia occupied the 9th position on a worldwide level and 2nd among men in order of frequency (2.7% registering 526 cases in the cancer compendium study run between 2000-2004); 429 patients were aged ≥60, that is 81.55% [4,5].

At the National Institute of Cancerology in Mexico, 50 to 70% of PC patients seek attention at an advanced stage; treatment is therefore aimed at improving life quality, following up on disease progression and safeguarding patients' general health.

Technological beak-through such as positron emission tomography using hybrid CT (PET/CT) equipment together with radiopharmaceuticals like 18F-NaF to detect metastatic, osteoblastic-type bone disease in PC [6,7], allow for methods that possess higher sensitivity as well as specificity rates (S: 86.7-100%; E: 44-88.6%) than bone scintigraphy (BS) (S: 82-99.8%; E: 19.4-66.5%).

CONTACT

Francisco O. García Pérez
Sevastián S. Medina Ornelas
Av. San Fernando, 22
Col. Sección XVI, Del. Tlalpan, C.P. 14080, México, D.F.
E-mail: dr.sevastian@outlook.com

The process of capturing this radiopharmaceutical from bone tissue is based on chemisorption with an exchange of ion 18F for ion [OH] at the surface of the hydroxyapatite matrix of the bone; it also forms fluorapatite and provokes the migration of 18F ions in crystals of the bone matrix. A minimum amount of bonding to proteins and fast renal clearance contribute to the high quality of images, with greater bone-depth proportions visible in shorter time-periods than those acquired with standard radiopharmaceuticals used for BS (99mTc-MDP) [8]. Recent publications point to 223Ra as an accepted treatment with castration-resistant prostate cancer patients where there is evidence of bone metastasis, no visceral metastasis, but persistent pain in the bones requiring radiotherapy or analgesics [11, 14, 16].

223Ra is high-energy alpha particle emitting radionuclide that selectively adheres to areas with greatest bone replacement during bone metastasis. [9]. It is concentrated in the bone due to its inclusion in hydroxyapatite crystals, where it replaces calcium during bone formation; it can also found on the circumference of metastatic areas [10]. Peak levels of bone absorption occur within 1 hour after injection, with no significant absorption changes found for the following 14 days, which indicates excellent bone tissue retention [12, 13].

There are to date, however, no studies to demonstrate whether positive clinical benefits can be attached to 223Ra in the treatment of bone metastases as found in hormone-sensitive PC.

CASE PRESENTATION

46-year old male with uneventful medical history seeks attention at the INCan in January 2014, presenting obstruction of urinary tract and overall bone pain symptoms (EVA 8), 220 ng/dl (APE) and 443 uds/L Alcaline Phosphate (AF), reason for which a biopsy is performed, where the histopathology report was as follows: Gleason 9 prostate adenocarcinoma (4+5) (figure 1).

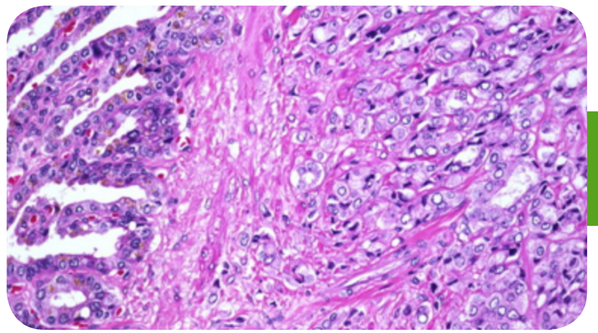

Figure 1. Biopsy of prostate report Gleason 9 prostate adenocarcinoma (4+5) [INCan Archive]

A Bone Scintigraphy (BS) was performed, reading: multiple osteoblastic-type bone metastases in axial and appendicular skeleton. An IV (AJCC) phase is declared; androgen deprivation therapy (ADT) is initiated using Bicalutamide and Gosereline as well as AINE, paracetamol and buprenorphine.

3 months following diagnosis the patient registered 26 ng/dl APE and 348 uds /l AF, with no pain-reduction reported but additional symptoms from side effects of therapy surfacing such as migraine, hot flashes, impotence and emotional lability. In order to assess the extent of the disease, a PET/CT scan was performed using SIEMENS mCT® equipment 30 min. after administering IV 10mCi of 18-NaF; the result indicated osteoblastic lesions in multiple axial and appendicular skeletal areas, where haematological values found within normal range.

PERIOD	WBC	HB	PLATELETS	NEUTROPHILS
Basal	5.5x109	14.8g/dL	323x109/L	5.4x103/uL
After 1° dose	5.3x109	14g/dL	330x109/L	5.1x103/uL
After 2° dose	5.3x109	14.4g/dL	325x109/L	4.9x103/uL
After 3° dose	5.0x109	14g/dL	310x109/L	4.4x103/uL
After 4° dose	4.66x109	13.7g/dL	301x109/L	4.1x103/uL

Table 1. More significant changes in the complete blood count (CBC)

With consent from the patient as well as from the Ethical Board of our institution, the latter ran a full evaluation and administered a first dose of IV 223Ra using 50KBq/kg

(3750KBq). Following a 30-day period and a haematological study, a second dose of 223Ra (3750KBq) was administered. A month later the patient reported a significant reduction in pain (EVA 2) and now required only paracetamol; there were likewise reductions in APE and AF levels, 4.8ng/dl and 128uds/L, respectively, as well as clear improvements with regard to side effects of ADT. A second PET/CT was performed using same characteristics and equipment as before, and here a decrease in blastic activity of metastatic lesions was noted (SUVmax) (figure 2-b); 24h later, following haematological control, a third doses of 223Ra is applied. After a fourth and prior to a fifth doses of 223Ra (3750KBq), a PET/CT was performed using same characteristics and equipment as before, with a significant decrease in the SUVmax of all metastatic lesions (figure 2-c); at this stage the patient reported almost no pain at all and ceased to require analgesics (EVA 1), indicating improvement in the quality of his life as well as low APE and AF levels: 0.133ng/dl and 48uds/L, respectively. The only relevant alterations were found in the neutrophilic count at 4.1x103/uL, and that of platelets at 301x109/L (table 1).

As well as the excellent response to pain shown by the patient and more favourable APE and AF levels registered at this stage of his treatment, he reported significant reductions in migraine and hot flashes generated by ADT therapy as from the 2nd doses of 223Ra administered.

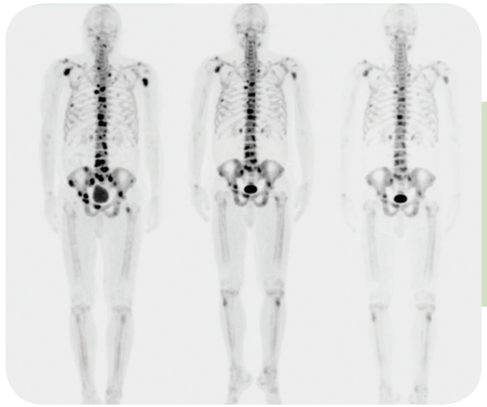

Figure 2. (a) PET/CT basal study using 18-NaF. (b) PET/CT with 18F-NaF following the administration of two 223Ra doses, (c) PET using 18F-NaF following the administration of four 223Ra doses.

The visual analogical scale provided by the WHO was used for the evaluation of pain; objective measurement of osteoblastic activity was based on SUVmax levels for the most representative lesions (figure 3); a BH was performed 24h prior to each application of therapy in order to monitor blood toxicity.

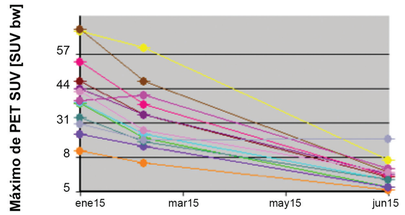

Figure 3. SUV max, behavior following 4 doses of treatment using 223Ra

CONCLUSION

With these preliminary results it may be concluded that a significant decrease in SUVmax levels for lesions caused by bone metastasis has been achieved using the PET/CT tool. The results have a correlation to APE and AF counts, where minimal effects produced in the patient's bone marrow and improvements in the quality of his life are equally noteworthy. Such data demonstrates the usefulness and effectiveness of 223Ra as an aiding agent that can be employed in conjunction with bicalutamide and gosereline to produce excellent results in treating patients with hormone-sensitive PC with symptomatic bone metastases; a further discovery was also made in the significant reduction of side effects generated by ADT therapy. The PET/CT study as conducted using 18F-NaF is a ground-breaking tool capable of substituting BS methods employed with 99mTc-MDP, since it allows for improved image quality and evaluation of SUVmax levels for each metastatic lesion following treatment with 223Ra.

ACKNOWLEDGEMENTS

Special thanks to Dr. Estrella A. Ramírez (Dalinde Medical Center, Mexico City) for reviewing the final article; likewise to the entire Department of Nuclear Medicine and Molecular Imaging (INCan) for providing its valuable services.

REFERENCES

1.- Ferlay J, Shin HR, Bray F, Forman D, Mathers C, Parkin DM. GLOBOCAN 2008 v1.
2, Cancer Incidence and Mortality Worldwide: IARC Cancer Base No. 10 [Internet]. Lyon, France: International Agency for Research on Cancer; 2010. 2.- A. Erazo-Valle, J. Martínez -Cedillo, S. Rivera-Rivera, et al. Reunión de panel de expertos en cáncer de próstata. Gaceta Mexicana de Oncología. 2014;13(Supl 2):2-17
3.- J.J. Sánchez-Barriga. Mortalidad por cáncer de próstata en México. Gaceta Médica de México. 2013;149:576-585
4.- Jiménez RM, Solares M, Martínez P, et al. Oncoguía: Cáncer de próstata. Cancerología 2011;6:13-18
5.- Rizo, et al. Registro Hospitalario de Cáncer: Compendio de Cáncer 2000 – 2004. Cancerología 2 (2007): 203-287
6.- De Jong IJ, Breeuwsma A J, Prium J, van der Jagt EJ, Jager PL, Nijman RJ et al. 18F sodium fluoride PET for the detection of bone metastases in prostate cancer. In: Prostate Cancer Symposium. 2006 ASCO
7.-. Avinash DL, Bal C, et al. The role of 18F-fluoride PET-CT in the detection of bone metastases in patients with breast, lung and prostate carcinoma: a comparison with FDG PET/CT and 99mTc-MDP bone scan. Jpn J Radiol (2013) 31:262–269
8.- Even-Sapir E, Metser U, Flusser G, Zuriel L, Kollender Y, Lerman H, et al. Assessment of malignant skeletal disease with 18Ffluoride PET/CT. J Nucl. Med. 2004;45:272–8
9.- Xofigo product information. U.S. Xofigo Web site. www.xofigo-us.com/productinformation.
10.- Neeta Pandit-Taskar, Steven M. Larson and Jorge A. Carrasquillo. Bone-Seeking Radiopharmaceuticals for Treatment of Osseous Metastases, Part 1: Therapy with 223Ra-Dichloride. J Nucl Med 2014; 55:268–274
11.- Prostate cancer. In National Comprehensive Cancer Network (NCCN) Clinical Practice Guidelines in Oncology, version 1.2015. National Comprehensive Cancer Network
12.- Nilsson S, Larsen RH, Fossa SD, et al. First clinical experience with alphaemitting radium -223 in the treatment of skeletal metastases. Clin Cancer Res.2005;11:4451–4459
13.- Carrasquillo JA, O'Donoghue JA, Pandit-TaskarN, et al: Phase I pharmacokinetic and biodistribution study with escalating doses of 223Ra dichloride in men with castration resistant metastatic prostate cancer. EurJ Nucl Med Mol Imaging 2013;40(9):1384-1393
14.- KluetzPG, PierceW, MaherVE, et al: Radium Ra223 dichloride injection: U.S. Food and Drug Administration drug approval summary. Clin Cancer Res2014;20(1):9-14
15.- A.S. Abi-Ghanem et al. Radionuclide Therapy for Osseous Metastases in Prostate Cancer. Semin Nucl Med. 2015; 45:66-80
16.- Parker C, Heinrich D, Helle SI, et al. Overall survival benefit and impact on skeletal-related events for radium-223 chloride (Alpharadin) in the treatment of castration-resistant prostate cancer (CRPC) patients with bone metastases: a phase III randomized trial (ALSYMPCA). Eur Urol Suppl. 2012;11:E130–U523. 17.- Coleman RE. Metastatic bone disease: clinical features, pathophysiology and treatment strategies. Cancer Treat Rev. 2001;27(3):165–76 18.- Larsen RH, Saxtorph H, Skydsgaard M, et al. Radiotoxicity of the alpha-emitting bone-seeker Ra-223 injected intravenously into mice: histology, clinical chemistry and hematology. In Vivo. 2006;20:325–331 19.- Withofs N, Grayet B, Tancredi T, Rorive A, Mella C, Giacomelli F, et al. 18F-fluoride PET/CT for assessing bone involvement in prostate and breast cancers. Nucl Med Commun. 2011;32(3):168–76 20.- Flamen P. Harnessing the Power of Collaboration for breast Cancer Research and treatment SNMMI Image of the Year Captured on the Discovery Pet/Ct 690 "IMAGE OF THE YEAR". MI clarity The magazine of molecular imaging. 2013; 12-14.

ABSTRACT

FEDERACION MEXICANA DE MEDICINA NUCLEAR CONGRESS, JUNE 2015

BONE LYMPHOMA MULTIFOCAL PRIMARY: FEATURES PET-CT AND MRI PRIOR TO TREATMENT

Dr. Serna, Dr. Quiroz, MD. Mateos, Dr. Galicia, Dr. Barrera.
PET-CT, Hospital Angeles del Pedregal

SUMMARY

Primary bone lymphoma, regardless its histological subtype is a rare find, with multifocal distribution being even less common. Primary bone lymphomas represent less than 5% of all bone tumors and 1% of cases of Non-Hodgkin Lymphomas (NHL). The broad spectrum of radiological features they can display make it easy to mislead diagnostic conclusions, thus, the proper analysis of history, imaging studies – such as MRI and PET-CT –, in addition to histopathological findings, become essential while assessing each case. We report here a case of Primary Bone Non-Hodgkin Lymphoma (PBNHL) diagnosed through bone marrow aspiration, along with its MRI and PET-CT findings, with subtle changes or unchanged by Computed Tomography.

DISCUSSION

Primary bone lymphoma (PBL) is an extranodal lesion arising from the medullary cavity, which manifests as a solitary localized lesion; it represents 3% of all malignant bone tumors and 1% of all malignant lymphomas. Formerly known as reticulum cell sarcoma, it was first described by Obeling in 1929, and was regarded as an extremely rare condition (1). PBL comprises 4 to 5% of extranodal lymphomas and 1% of all NHL (2).

According to the World Health Organization, lymphomas that affect bone tissue can be divided into four groups: Group 1 includes lymphomas affecting a single bone with but without lymph node affection; Group 2, lymphomas with multiple lesions and without visceral or lymph node affection – the present case belonging to this group –; Group 3, bone tumors with visceral or lymph node affection at single or multiple sites; and Group 4, lymphomas affecting other sites and intentionally found in a bone biopsy (2). To define NHL as bone-originated, it must meet Coley's criteria: 1) primary focus on a single bone. 2) positive histological diagnosis, and 3) no evidence of affection or infiltration to soft tissue (6).

This type of tumor occurs between the ages of 20-50, having a higher prevalence in men with a ratio of 3:2 with respect to women. The femur is affected 29% of the time, followed by pelvic bones (19%), humerus (13%), skull (11%), and tibia (10%). It is noteworthy that both long bones and flat bones are affected evenly (3).

Clinical presentation is non-specific, occurring as intermittent and insidious bone pain – similar to that of spinal cord compression – which usually persists for months, along with weight loss and fever. In 50% of cases, the pain is associated with a painful palpable edematous mass (4. 5).

Cell morphology is histopathologically indistinguishable from nodal lymphoma and non-Hodgkin lymphoma derivatives. Microscopy shows a mixture of large cells of B-cell lineage, with 75% classifiable as intermediate, diffuse or mixed degree, and may display a herringbone morphology.

Radiologically, presentation is variable and may involve any part of the skeleton with non-specific signs on imaging studies (1). In this patient, the lesion appeared as a normal pattern without detectable injuries in radiography or CT, an uncommon presentation, since the most usual form – reported in 70% of the cases – is a destructive lytic pattern, which is described as permeative, featuring numerous elongated lesions parallel to the long axis of the bone. They also display a spotted pattern and well defined margins, with pathological fractures happening 25% of the time, along with loss of cortex. Periosteal reactions happen in 60% of the cases, with a layered or "onion" appearance that can be continuous or discontinuous – the latter bearing a worse prognosis.

MRI is used to detect local invasion of bone marrow and to evaluate the extent of it. The T1 sequence is best for detecting bone marrow changes. Affected areas appear bright in T2 sequence due to peritumoral edema. Fibrosis, if there is any, will appear as a low intensity lesion and may be enhanced after administration of contrast medium. MRI also allows viewing of important cortical erosion sites in affected soft tissue.

It is known that CT with FDG PET in lymphoma has higher sensitivity for lesion detection than conventional imaging methods, where tracer uptake is correlated with the lymphoma's metabolic activity aggressiveness (7). In the context of bone tumors, this method has also been proven to be sensitive and specific when compared to conventional imaging when used to detect bone involvement (8). In a meta-analysis conducted in 2012, where PET, PET-CT and MRI were compared, it was observed that sensitivity is significantly higher for FDG-PET-CT (estimated around 91.6%, with a specificity of 90.3%) when compared to MRI (with 90.3% sensitivity and 75.9% sensitivity) (9). In another study published in 2014, where the role of B-cell lymphoma was evaluated, it was found that PET CT FDG is a complementary study to the detection of bone lesions. In this study, a positive scan was shown to render biopsy unnecessary (10). At this point it is important to emphasize that the correct staging of the disease is crucial before treatment is selected.

Different nuclear medicine tracers have been investigated and compared with conventional imaging methods in patients with PBL. Stroszczynski et al. It found that Ga67 has a 70% sensitivity and 93% specificity when evaluating primary bone tumor activity in lymphoma. MRI findings which showed a 90% sensitivity with an 80% specificity (11).

When evaluating the stages of bone lymphoma, classification by Murphy is used. Stage I refers to a localized disease. In stage II, a single bone is involved and local ganglia are compromised. In stage III, several bone sites are affected, but bone marrow and lymph nodes remain uncompromised. This patient meets the criteria for classification as stage III, thus chemotherapy is the treatment of choice (12).

CONCLUSION

PBL is a rare and difficult entity to recognize because diagnosis is reached through the exclusion of other entities in the differential diagnosis. Radiographic findings are variable and nonspecific, appearing in a wide spectrum ranging from subtle changes to the expansive lytic lesions. In the case hereby studied, the patient's radiographic pattern was a subtle and near normal one. This pattern is of particular interest due to the absence alteration in radiographs – and even in CT – with surprising appearance of lesions in MRI, scintigraphy and hybrid techniques such as PET-CT. The latter provides a crucial assessment of metabolic activity for diagnosis, staging and follow-up.

REFERENCES

Pickard, M. "FAU (Finkel-Biskis-Reilly murine sarcoma virus (FBR-MuSV) ubiquitously expressed)", Atlas Genet Cytogenet Oncol Haematol, 2012; 16(1): 12-17.

Welling MM, Ferro-Flores G, Pirmettis I, Brouwer C. "Current Statutus of imaging infections with radiolabeled anti-infective agents", Anti-Infective Agents in Medicinal Chemistry, 2009; 8 (3):272-287.

Welling MM, Lupetti A, Balter HS, et.al. 99m-Tc labeled antimicrobial peptides for detection of bacterial and Candida albicans infections", J Nucl Med 2001; 42;788-794.

Saeed A, Iqbal J, Hkan M, et.al. "99m Tc labeled antimicrobial peptide ubiquicidin (29-41) accumulates less in Escherichia coli infection tan in Staphlococcus aureus infection", J Nucl Med 2004; 45:849-856.

Brouwer C, Gemmel F, Welling MM. " Evaluation of 99m Tc-UBI 29-41 scintigraphy for specific detection of experimental multidrug-resistant Staphylococcus aureus bacterial endocarditis", Q J Nucl Med 2010; 54(4);442-450

Ferro-Flores G, Arteaga de Murphy C, Pedraza-López M, et.al. "In vitro and in vivo assesment of 99m Tc UBI specificity for bacteria", Nucl Med Biol, 2003; 30(6):597-603.

Hancock REW, Scott MG. "The role of antimicrobial peptides in animal defenses", Proc Natl Acad Sci 2000; 97:55.

Lupetti A, Welling MM, Pauwels EK, Nibbering PH."Detection of fungal infections using radiolabeled antifungal agents", Curr Drug Targets, 2005; 6(8):945-954.

Lupetti A, Pauwels EKJ, Nibbering PH, Welling MM. "99m Tc- Antimicrobial peptides: Promising candidates for infection imaging", Q J Nucl Med 2003; 47:238-245.

Crudo JL, Nevares NN, Zapata AM, et.al. "Un estudio completo sobre la obtención de 99mTc-UBI 29-41 y su comportamiento in vitro e in vivo: su potencial uso en imágenes de infecciones", Alasbimn Journal 2005;7(28)

Ferro-Flores G, Arteaga de Murphy C, Melendez-Alafort L, et.al. "Molecular recognition and stability of 99mTc UBI 29-41 based on experimental and semiempirical results", Appl. Radiat. Isot, 2004: 61: 1261-1268.

Melendez-Alafort L. Ramirez Fde M. Ferro-Flores G. Arteaga de Murphy C. Pedraza-Lopez M. Hnatowich D.J. "Lys and Arg in UBI: a specific site for a stable Tc-99m complex?" Nucl Med Biol 2003;30(6):605–15.

Beiki D, Yousefi G, Fallahi B, et.al. "99m Tc-ubiquicidin 29-41, a promising radiopharmaceutical to differentiate orthopedic implant infections from sterile inflammation", Iranian Journal of Pharmaceutical Research, 2013, 12(2): 347-353

Ostovar A, Assadi M, Vahdat K, et.al. "A pooled analysis of diagnostic value of 99m Tc-ubiquicidin (UBI) scintigraphy in detection of an infectious process", Clin Nucl Med 2013; 38(6):413-416

Peschel A. "How do bacteria resist human antimicrobial peptides?", Trends Microbiol, 2002; 10:179-186

99mTc-Ubiquicidin29-41, Molecular Imaging & Contrast Agent Database.

Saeed S, Zafar J, Khan B, et.al. "Utility of 99m-Tc labelled antimicrobial peptide ubiquicidin (29-41) in the diagnosis of diabetic foot infection", Eur Nucl Med Mol Imaging 2013; 40(5):737-743.

Taghizadesh M, Mandegar M, Assadi M, "Technetium-99m-ubiquicidin scintigraphy in the detection of infective endocarditis", Hell J Nucl Med 2014; 17(1);47-48.

Sepúlveda-Mendez J, Arteaga de Murphy C, Rojas-Bautista JC, Pedraza-López M, "Specificity of 99mTc-UBI for detecting infection foci in patients with fever in study", Nucl Med Commun 2010; 31:889-895.

NUM 2

VOL 2 + MAY - AUGUST 2015